Rotation of a two-dimensional Coulomb cluster in a magnetic field

Osamu Ishihara
Faculty of Engineering, Yokohama National University, Yokohama 240-8501, Japan

Tetsuo Kamimura and Keiichi I. Hirose
National Institute for Fusion Science, Toki 509-5292, Japan

Noriyoshi Sato
Graduate School of Engineering, Tohoku University, Sendai 980-8579, Japan
(Received 26 October 2001; published 10 October 2002)

A coordinated study of a laboratory experiment, a computer simulation, and a theoretical analysis reveals a structure and its dynamic motion of a Coulomb cluster trapped in a plasma with a confining potential in the presence of gravitational and magnetic fields. Charged dust particulates are found to form a circle in a horizontal plane with a radius determined by a balance of a restoring force due to a confining potential and the screened Coulomb force between dust particulates. The dust particulates in a circle show angular rotation with the structure intact, while they oscillate radially around the equilibrium orbit. The analytical study reveals the oscillatory rotational nature of dust particulates as a result of coupling between the Lorentz force and the harmonic oscillation.

DOI: 10.1103/PhysRevE.66.046406 PACS number(s): 52.27.Lw

I. INTRODUCTION

Since the observation of plasma crystal formation in 1994, behavior of fine particles, ranging from submicron to tens of microns in size, ubiquitously present in plasmas in space as well as in laboratory has been extensively studied by experiments, simulations, as well as theories [1]. Such particulates, called fine particles, grains, or dust particulates are charged negatively, typically with 10^3–10^4 electronic charges, in a plasma as a result of balancing electron and ion flux flowing onto the surface. Such a large charge substance in a plasma modifies the basic properties of a plasma like a Debye length and shows a unique feature such as formation of a wake potential in the presence of ion flow [2,3]. The presence of a large number of dust particulates in a plasma develops new types of collective phenomena including low frequency oscillations, waves, and instabilities [4]. The structure of a cloud with a large number of dust particulates was successfully controlled by the application of an external potential in dc discharge plasmas [5]. Recent observations of the rotation of a cloud of dust particulates in the presence of a magnetic field stimulate further interest in the physics of dusty plasmas [6,7] and a spinning motion of a dust particulate in the cloud was also studied [8]. The rotation of a Coulomb cluster in a plasma has been studied theoretically in which ion-neutral collisions play a major role associated with the ion $\mathbf{E}\times\mathbf{B}$ driving force [6,9]. However, the detailed experimental observation of the rotation of a small number of dust particulates in a magnetic field revealed the radial oscillatory motion along the circular orbit as reported in Ref. [7]. Such a dynamic behavior of the dust particulates motivates us to propose a mechanism of cluster rotation in a plasma in the presence of magnetic field. In this paper, analytical study shows dynamical behavior of a Coulomb cluster in the presence of magnetic field, in support of the experimental observation and the particle simulation.

II. DYNAMIC EQUATIONS

The dynamics of dust particulates forming a polygon structure in a horizontal plane in the presence of gravitational and magnetic fields may be described by a Hamiltonian

$$H=\frac{1}{2M}\left|\mathbf{p}-\frac{Q}{c}\mathbf{A}\right|^2+V(\mathbf{r},z), \tag{1}$$

where $V(\mathbf{r},z)$ is an external potential described as

$$V(\mathbf{r},z)=\tfrac{1}{2}K_1r^2+\tfrac{1}{2}K_2z^2+Q\phi+Mgz. \tag{2}$$

Here Q and M are charge and mass of a dust particulate, respectively;

$$\mathbf{A}=(A_r,A_\theta,A_z)=(0,rB/2,0) \tag{3}$$

is the vector potential assuming the z directional magnetic field, K_1 and K_2 are constants to define a confining potential, $r^2=x^2+y^2$, Mgz is a gravitational potential, and ϕ is the screened Coulomb potential defined by

$$\phi=\sum_j\frac{Q}{|\mathbf{r}-\mathbf{r}_j|}\exp\left(-\frac{|\mathbf{r}-\mathbf{r}_j|}{\lambda_D}\right), \tag{4}$$

where λ_D is the Debye length and the summation is taken for all the neighboring dust particulates. We note that our generalized force $\mathbf{F}^G$ may contain a force $\mathbf{F}$ not derivable from potentials, including the ion drag force and the frictional force by neutral particles, or

$$F^G=-\nabla V+\mathbf{F}. \tag{5}$$

The momenta are given through

$$\dot{q}_j=\frac{\partial H}{\partial p_j}\ (q_j=r,\theta,z) \tag{6}$$

as

$$p_r = M\dot{r}, \tag{7}$$

$$p_\theta = Mr^2\dot{\theta} + Qr^2B/2c, \tag{8}$$

$$p_z = M\dot{z}, \tag{9}$$

where a dot indicates the differentiation with respect to time. The Hamilton equations of motion for a dust particulate with a generalized force in consideration are given through

$$\dot{p}_j = -\frac{\partial H}{\partial q_j} + F_j, \tag{10}$$

as

$$\dot{p}_r = Mr\dot{\theta}(\dot{\theta} + \omega_c) - K_1 r - Q\partial\phi/\partial r + F_r, \tag{11}$$

$$\dot{p}_\theta = -Q\partial\phi/\partial\theta + rF_\theta, \tag{12}$$

$$\dot{p}_z = -K_2 z - Q\partial\phi/\partial z - Mg + F_z, \tag{13}$$

where $\omega_c = QB/Mc$. The force due to the ion drag and the neutral friction may be expressed as

$$\mathbf{F} = -M[(\mathbf{v}_d - \mathbf{v}_i)/\tau_i + (\mathbf{v}_d - \mathbf{v}_n)/\tau_n], \tag{14}$$

where $\mathbf{v}_d$, $\mathbf{v}_i$, and $\mathbf{v}_n$ are the velocities of a dust particulate, an ion, and a neutral particle, respectively, and τ_i and τ_n are the characteristic times for ion drag and the neutral friction. The characteristic times are expressed as

$$\tau_i = \frac{M}{m_i n_i \langle v_i \rangle \sigma_i} \tag{15}$$

and

$$\tau_n = \frac{3M}{4\pi r_d^2 m_n n_n \langle v_n \rangle}, \tag{16}$$

where subscripts i and n indicate ions and neutral particles, m is mass, n is number density, $\langle v \rangle$ is the mean speed, σ_i is the cross section for ions, and r_d is the radius of a spherical dust particulate [10,11]. The characteristic times of ion drag and neutral friction are rather slow because of heavy nature of a dust particulate. For a spherical dust particulate of $r_d \sim 1\ \mu$m and $M \sim 4\times10^{-15}$ kg with $n_i \sim 10^{15}\ \mathrm{m}^{-3}$, $n_n \sim 10^{21}\ \mathrm{m}^{-3}$, $\langle v_i \rangle \sim 500\ \mathrm{m\,s}^{-1}$, $\langle v_n \rangle \sim 10\ \mathrm{m\,s}^{-1} \gg |\mathbf{v}_d|$, and $\sigma_i \sim 10^{-8}\ \mathrm{m}^2$, the characteristic times are estimated to be $\tau_n \sim \tau_i \gtrsim 10$ sec in argon plasma and $\tau_n \sim \tau_i \approx 10$ min for hydrogen plasma. The thrust in the present paper is on the dynamics of dust particulates in magnetic field, and our analysis starts without the ion drag and the neutral friction. The effects of the ion drag and the neutral friction will be discussed later.

III. RING STRUCTURE OF A COULOMB CLUSTER

Now we consider n dust particulates equally spaced near a horizontal circle at $z = z_0$ plane with radius r_0. The coordinate of the ith dust particulate is given by [11]

$$\mathbf{r}_i = r_0(\cos\theta_i \mathbf{e}_x + \sin\theta_i \mathbf{e}_y) + z_0\mathbf{e}_z + \delta\mathbf{r}_i, \tag{17}$$

where

$$\theta_i = \frac{i2\pi}{n} + \delta\theta_i \tag{18}$$

and $\delta\mathbf{r}_i$, $\delta\theta_i$ are the radial and angular deviations from the equilibrium position. We note that the vertical perturbations induced by the coupling with neighbor particles are responsible for the stability of the structure as discussed in Ref. [11]. The equilibrium radius depends on the number of dust particulates in a circle and can be found from the time-independent equation

$$-K_1 r - Q\partial\phi/\partial r = 0 \tag{19}$$

with $\delta\theta = 0$ as

$$r_0 = \alpha_n r_K, \tag{20}$$

$$\alpha_n = \left[\frac{\sqrt{3}}{4} \sum_{j=1(j\neq i)}^{n} \frac{e^{-2r_0|\sin(\theta_{i-j}/2)|/\lambda_D}}{|\sin(\theta_{i-j}/2)|} \times \left(1 + \frac{2r_0}{\lambda_D} \frac{|\sin(\theta_{i-j}/2)|}{\sin(\theta_{i-j}/2)} \right) \right]^{1/3}, \tag{21}$$

$$r_K = \left(\frac{Q^2}{\sqrt{3}K_1} \right)^{1/3}. \tag{22}$$

The numerical values are $\alpha_n = 1$ $(n=3)$, 1.18 $(n=4)$, 1.34 $(n=5)$, and 1.47 $(n=6)$ in the long shielding limit. These values will be examined by the laboratory experiment as well as by the simulation.

IV. EQUATIONS OF MOTION

Now we consider a situation away from the equilibrium. The equations of motion for the ith particulate give the following equations:

$$M\delta\ddot{r}_i = M(r_0 + \delta r_i)\delta\dot{\theta}_i(\delta\dot{\theta}_i + \omega_c) - 3K_1\delta r_i + \frac{Q^2}{4r_0^2}\sum_{j\neq i}\delta f_1(\theta_{i-j}), \tag{23}$$

$$M(r_0 + \delta r_i)\delta\ddot{\theta}_i + 2M\delta\dot{r}_i\delta\dot{\theta}_i + M\omega_c\delta\dot{r}_i = \frac{Q^2}{4r_0^2}\sum_{j\neq i}\delta f_2(\theta_{i-j}), \tag{24}$$

where $\delta f_1(\theta_{i-j})$ and $\delta f_2(\theta_{i-j})$ are the screened Coulombic perturbations induced by the interaction with other particulates in the circle. We note that Eq. (20) was used in deriving

Eq. (23). The simultaneous equations given by Eqs. (23) and (24) for $i=1\sim n$ describe the behavior of n particulates in the circle. Although dust particulates in the circle are strongly coupled through the screened Coulomb force, the individual behavior of the ith particulate may well be described by the coupling of Eqs. (23) and (24) in the weak coupling limit where the screened Coulombic perturbations may be negligible. To analyze dynamic motion of the ith dust particulate in the circle, we introduce normalized quantities $R=r_i/r_0=|\mathbf{r}_i|/r_0$, $T=\omega_p t$, $\Omega=\omega_i/\omega_p=\dot{\theta}_i/\omega_p$, and $\Omega_c=\omega_c/\omega_p$, where

$$\omega_p=(3K_1/M)^{1/2}. \tag{25}$$

Noting that $\delta\dot{r}_i=\dot{r}_i$ and $\delta\dot{\theta}_i=\dot{\theta}_i=\omega_i$ we find normalized equations

$$\ddot{R}=R\Omega(\Omega+\Omega_c)-(R-1), \tag{26}$$

$$R\dot{\Omega}+2\dot{R}\Omega+\Omega_c\dot{R}=0. \tag{27}$$

Since the left hand side of Eq. (27) can be written as $(1/R)d[R^2(\Omega+\Omega_c/2)]/dT$, we find that

$$R^2\left(\Omega+\frac{\Omega_c}{2}\right)=h\equiv a^2\left(\Omega_0+\frac{\Omega_c}{2}\right), \tag{28}$$

where a is the normalized initial radial displacement and Ω_0 is the normalized initial angular frequency of a dust particulate. On the other hand, Eq. (26), by multiplying $2\dot{R}$ on both sides and integrating with respect to time, leads to

$$\frac{dR}{dT}=\pm\sqrt{2[E-U(R)]-\frac{h^2}{R^2}}, \tag{29}$$

where $U(R)=(1+\Omega_c^2/4)R^2-2R$ and E is a constant given by $E=[\dot{R}^2/2+h^2/2R^2+U(R)/2]_{t=0}$. Equations (28) and (29), by noting $\Omega=d\theta_i/dT$, give the relation between the angle θ for the ith particulate and the radial displacement R as

$$\theta(R)=\theta_0\pm\int_a^R\frac{2h-\Omega_c r^2}{2r\sqrt{2r^2[E-U(r)]-h^2}}dr, \tag{30}$$

where θ_0 is the initial angle for $R=a$. The trajectories of a dust particulate initially located at $\theta=\theta_0=0$ are described by Eqs. (26) and (27) and are shown in Fig. 1 in the x-y plane for $\Omega_c=-0.1$ with various initial conditions of a and Ω_0. The criterion for the direction of the rotation can be found by setting $R=1$ in Eq. (28) and is described by a parameter W defined by

$$W=\Omega_0+\left(1-\frac{1}{a^2}\right)\frac{\Omega_c}{2}. \tag{31}$$

The rotation is counterclockwise if $W>0$ and clockwise if $W<0$. Figures 1(a), 1(d), and 1(e) show the counterclockwise rotation for $W>0$, while Figs. 1(b), 1(c), and 1(f) show

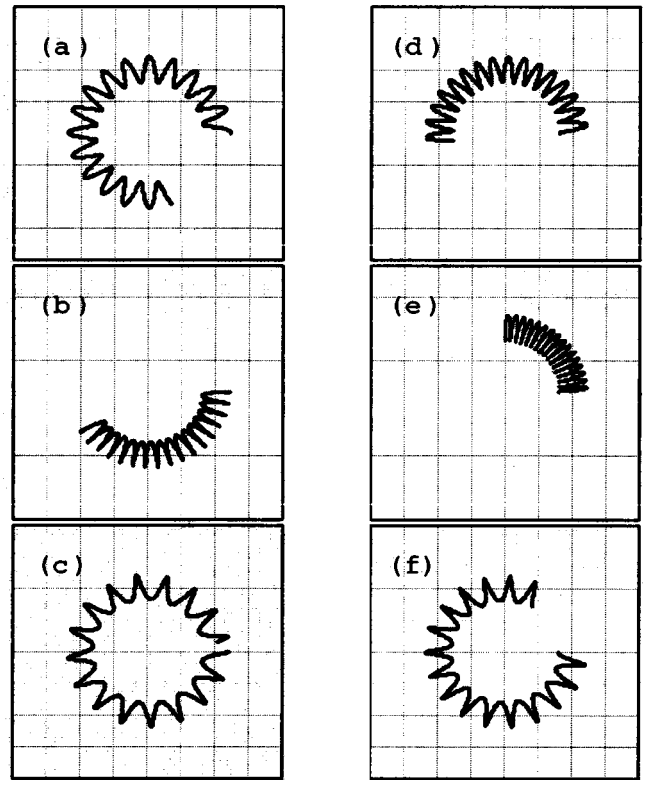

FIG. 1. Trajectories of a dust particulate in the magnetic field ($\Omega_c=-0.1$) as described by Eqs. (26) and (27). A dust particulate is initially placed at $\theta=\theta_0=0$ with radius $R=a$ and initial frequency $\Omega=\Omega_0$. (a) $a=1.2$, $\Omega_0=0.05$, $W=0.03$; (b) $a=1.2$, $\Omega_0=0$, $W=-0.02$; (c) $a=1.2$, $\Omega_0=-0.025$, $W=-0.04$; (d) $a=0.8$, $\Omega_0=0.025$, $W=0.05$; (e) $a=0.8$, $\Omega_0=0$, $W=0.03$; (f) $a=0.8$, $\Omega_0=-0.1$, $W=-0.07$.

the clockwise rotation for $W<0$. From the temporal evolution of the angle θ the average angular rotational frequency Ω can be evaluated. Figure 2 shows the time-average angular frequency of the particulate as a function of the magnitude of cyclotron frequency Ω_c for $a=1.2$ and $\Omega_0=0$. Equations (28) and (26) can be used to evaluate the asymptotic equations by setting $R\simeq 1$ for $\Omega_c\ll 1$ and $\ddot{R}\simeq 0$ for $\Omega_c\gg 1$. In the weak and strong field limits the angular frequencies are given by

$$\Omega=\tfrac{1}{2}(a^2-1)\Omega_c \quad \text{for} \quad \Omega_c\ll 1, \tag{32}$$

$$\Omega=-\frac{1}{2a^2(2\Omega_0+\Omega_c)}+\frac{1}{2\Omega_c} \quad \text{for} \quad \Omega_c\gg 1. \tag{33}$$

The asymptotic angular frequencies given by Eqs. (32) and (33) are shown in Fig. 2. The angular frequency shows a minimum when the magnitude of the cyclotron frequency is ≈ 0.7. Equations (32) and (33) show that the angular frequency vanishes when $a=1$ and $\Omega_0=0$, indicating that the dust rotation stops when frictional forces are present. The angular motion, driven by the coupling of Lorentz force and harmonic oscillation, will slow down in a time scale of the characteristic times of the ion drag and the neutral friction,

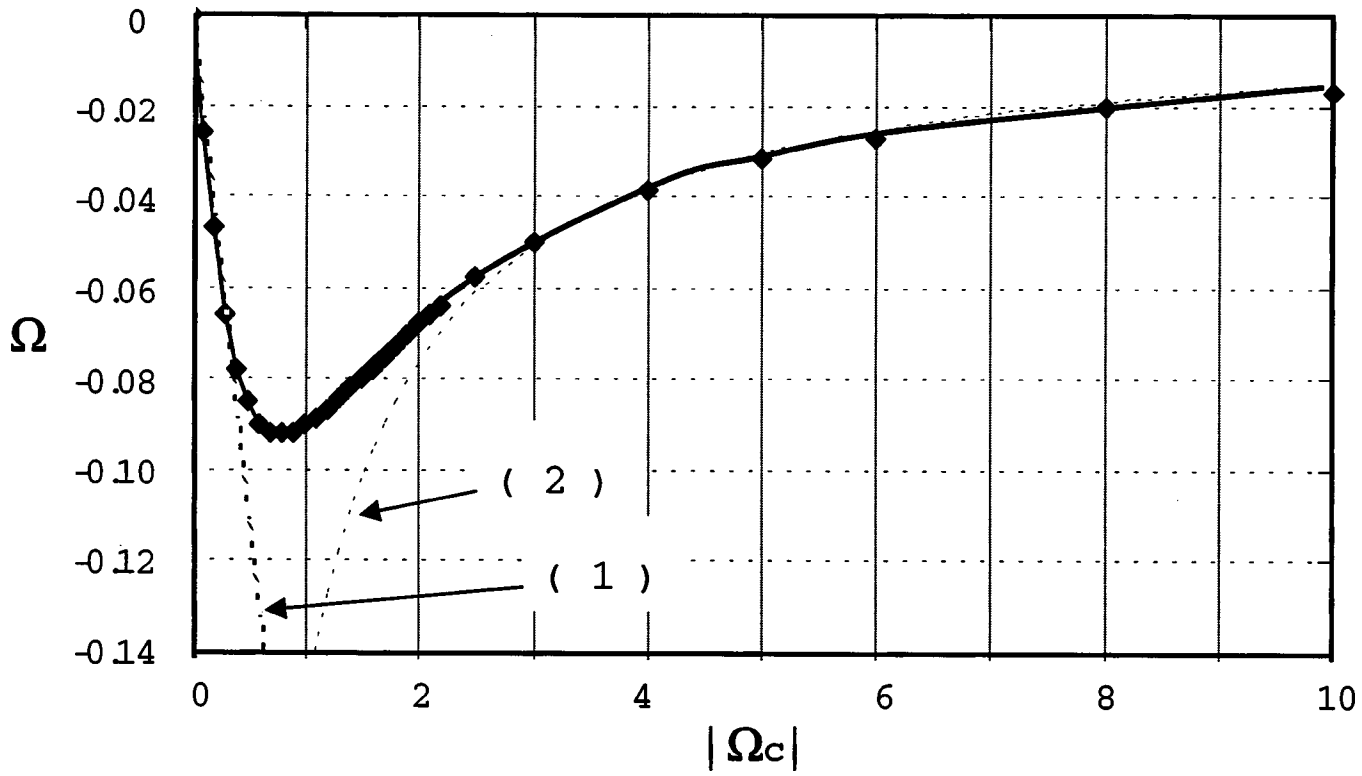

FIG. 2. The time-average angular frequency, Ω, vs the magnitude of the cyclotron frequency, $|\Omega_c|$ as described by Eqs. (26) and (27). (1) A weak field limit given by Eq. (32). (2) A strong field limit given by Eq. (33).

and that is when the azimuthal drift of the dust particulate is expected to be stimulated by the azimuthal drift of ions in crossed radial electric field and vertical magnetic field as described in Ref. [6]. Once dust particulates are pushed away from the equilibrium position, i.e., $a \neq 1$, the Lorentz force coupled with the harmonic oscillation will take over the dynamics of the motion of dust particulates.

V. EXPERIMENT

In a laboratory experiment, a group of dust particulates is observed to form a polygon structure in an externally imposed potential in a dc discharge argon plasma of the plasma density around 10^8 cm^{-3}, the electron temperature of a few eV with a gas pressure of 220–260 mTorr. The parabolic confining potential has a potential hill to confine negatively charged dust particulates and is formed at about several millimeters above the levitation electrode with a radial spread of about 1 cm by a method described in Ref. [7]. The cluster forming a polygon structure could be as simple as a triangle, a square, a pentagon, and a hexagon, and could develop into a cluster of polygons, a plasma crystal, when dust particulates are increased in number in the confining potential. Figures 3(a–c) show the observed polygon structures of dust particulates in the dc discharge. The structures are formed by injecting methyl methacrylate polymer spheres of 0.05 $\sim$5 μm in radius with a specific gravity of around 1 g/cm^3 into the confining parabolic potential under the gravity. A typical polygon radius is on the order of 0.1 to a few millimeters depending on the dust particulate radius, charge, and the strength of the confining potential. The ratios of the radii for various polygon structures, thus observed, agree well with the analytical predictions given by Eq. (20), except for the cases of $n=6$ and higher values of n. The observed radius for $n=6$ is somewhat larger than the value predicted by Eq. (20). This is because the sixth dust particulate is settled in the center of the circle, which is not incorporated in our analytical model. The experiment shows the rotation of the particulates consisting of a polygon in the presence of a vertical magnetic field of up to 0.4 kG (see Fig. 5 of Ref. [7]). Because of the difficulty of experimental conditions to produce a stable symmetric plasma in the presence of a strong magnetic field in a dc discharge, the dynamic motion of the dust particulates is studied in a rf discharge plasma for the magnetic field up to 40 kG. The stable discharge was still difficult to produce even in a rf plasma in a strong magnetic field above 10 kG. The angular frequency of the rotating cluster is found to increase linearly with the field strength up to about 3 kG and saturates in its magnitude followed by the decrease of the frequency for the strong field above about 8 kG (see Figs. 9 and 10 of Ref. [7]). Such a linear dependence on magnetic field in the weak field regime and the saturation followed by the decrease of the angular frequency are well described by our analytical model as shown in Fig. 2. The rotational direction was controlled by changing the polarity of the external electric field which modifies the radial structure of the confining potential, corresponding to the change of the parameter W or initial conditions as described by Eq. (31). The experimental observation revealed the oscillatory

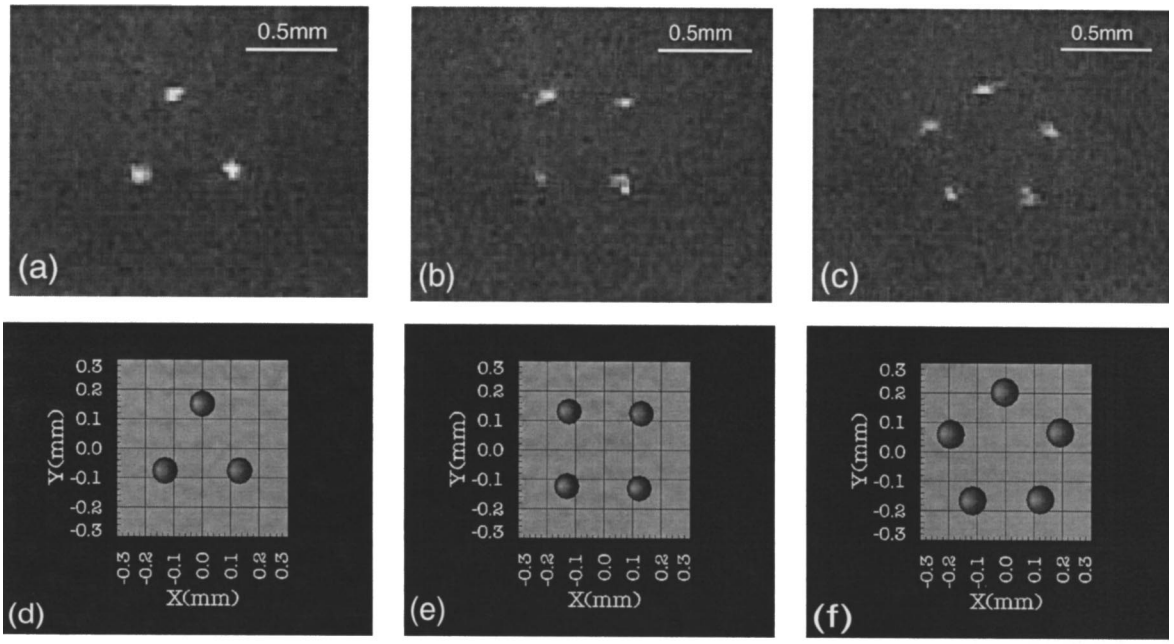

FIG. 3. Polygon structures of dust particulates in the horizontal plane in argon plasma. (a)–(c) Laboratory experiment with dust particulates of 5 μm radius with specific gravity of 1.20 g/cm^3. (d)–(f) Simulation results.

orbiting motion of dust particulates as shown in Fig. 6 of Ref. [7], a unique feature shown theoretically in Fig. 1.

VI. PARTICLE SIMULATION

A two-dimensional particle simulation is performed to model the formation of plasma crystals in the presence of electric and magnetic fields. Charged dust particulates are assumed to have radius 5.0 μm, mass 6.2×10^{-13} kg, and charge 1.6×10^{-14} C. A confining potential U is assumed to have a quadratic form, $U=K_1r^2/2$, where r is the horizontal radial distance from the center of the system under consideration and a constant $K_1(=6\times10^5$ eV/cm$^2)$ is chosen to reproduce the experimental conditions. A small number of charged dust particulates are introduced in the system, and trapped in the confining potential under the action of Coulomb force between dust particulates as well as a prescribed frictional force ($\mathbf{F}=-\mu\dot{\mathbf{r}}, \mu=0\sim1.5\times10^{-11}$ kg/sec) due to ions and neutral particles. The simulation model and preliminary results were reported earlier [12]. The simulation shows the polygon structure for dust particulates in equilibrium as was observed in the experiment. Figures 3(d), 3(e), and 3(f) show the results of simulation with $\mu=1.5\times10^{-11}$ kg/sec, in which the ratios of the radii are in good agreement with the analytical prediction given by Eq. (20). Further introduction of dust particulates in the confining potential formed a cluster of dust particulates. In the presence of magnetic field ($\sim$400 G) perpendicular to the two-dimensional plane without frictional force ($\mu=0$), the simulation shows the orbital angular motion of dust particulates along the equilibrium orbit with some perturbations of radial oscillatory nature. Even with the rotation, the polygon structure of dust particulates remains the same at any given time. The simulation result suggests that the dust angular rotation is not simply due to the Lorentz force, but due to the coupling of the Lorentz force with a restoring force to keep the particulates in equilibrium orbit. The simulation supports the mechanism proposed by the analytical picture presented in this paper.

VII. CONCLUSIONS

In conclusion, the equilibrium condition and the dynamics of polygon structures of dust particulates confined in a potential in the presence of gravitational and magnetic fields are well understood by a coordinated study of laboratory experiment, particle simulation, and the analytical theory. Theory based on Hamilton equations of motion reveals that dust particulates form polygon structures in a horizontal plane with dynamic motion of angular rotation accompanied by radial oscillation with the structure intact. The theory also shows the rotational direction of dust particulates as a result of the coupling of the Lorentz force and the harmonic oscillation. The rotational frequency is found to be linear with the weak magnetic field, although the frequency is inversely proportional to the field in the strong field limit.

ACKNOWLEDGMENT

This work was partly supported by the Grants-in-Aid for Scientific Research (C) program of the Japan Society for the Promotion of Science.

[1] For example, *Physics of Dusty Plasmas*, edited by M. Horanyl, S. Robertson, and B. Walch (AIP, New York, 1998); *Frontiers in Dusty Plasmas*, edited by Y. Nakamura and T. Yokota, and P. K. Shukla (Elsevier Science, Amsterdam, 2000).

[2] J.R. Sanmartin and S.H. Lam, Phys. Fluids **14**, 62 (1971); L. Chen, A.B. Langdon, and M.A. Lieberman, J. Plasma Phys. **9**, 311 (1973).

[3] M. Nambu, S.V. Vladimirov, and P.K. Shukla, Phys. Lett. A **203**, 40 (1995); S.V. Vladimirov and O. Ishihara, Phys. Plasmas **3**, 444 (1996); O. Ishihara and S.V. Vladimirov, *ibid.* **4**, 69 (1997).

[4] For example, P.K. Shukla, Phys. Plasmas **8**, 1791 (2001).

[5] N. Sato, G. Uchida, R. Ozaki, S. Iizuka, and T. Kamimura, in *Frontiers in Dusty Plasmas*, edited by Y. Nakamura, T. Yokota, and P.K. Shukla (Elsevier, Amsterdam, 2000), pp. 329–336.

[6] U. Konopka, D. Samsonov, A.V. Ivlev, J. Goree, V. Steinberg, and G.E. Morfill, Phys. Rev. E **61**, 1890 (2000).

[7] N. Sato, G. Uchida, T. Kaneko, S. Shimizu, and S. Iizuka, Phys. Plasmas **8**, 1786 (2001).

[8] O. Ishihara and N. Sato, IEEE Trans. Plasma Sci. **29**, 179 (2001).

[9] P.K. Kaw, K. Nishikawa, and N. Sato, Phys. Plasmas **9**, 387 (2002).

[10] P.S. Epstein, Phys. Rev. **23**, 710 (1924).

[11] O. Ishihara, Phys. Plasmas **5**, 357 (1998).

[12] T. Kamimura, K. Hirose, G. Uchida, S. Iizuka, and N. Sato, J. Plasma Fusion Res. **4**, 480 (2001).